alexpacini.com

Design of a Position-Independent End-to-End Inductive WPT Link for Industrial Dynamic Systems

Alex Pacini, Alessandra Costanzo, S. Aldhaher, and P. D. Mitcheson

Author Accepted Manuscript

To cite this version:

A. Pacini, A. Costanzo, S. Aldhaher, and P. D. Mitcheson, "Design of a Position-Independent End-to-End Inductive WPT Link for Industrial Dynamic Systems," in *2017 IEEE MTT-S International Microwave Symposium (IMS)*, Jun. 2017, pp. 1053–1056, doi: 10.1109/MWSYM.2017.8058774.

```
@inproceedings{Pacini_2017_IMS_PositionIndependent,
  author    = {Alex Pacini and Alessandra Costanzo and S. Aldhaher and P. D. Mitcheson},
  title     = {Design of a Position-Independent End-to-End Inductive WPT Link for
               Industrial Dynamic Systems},
  booktitle = {2017 IEEE MTT-S International Microwave Symposium (IMS)},
  year      = {2017},
  pages     = {1053--1056},
  month     = jun,
  doi       = {10.1109/MWSYM.2017.8058774}
}
```

© 2017 IEEE. Personal use of this material is permitted. Permission from IEEE must be obtained for all other uses, in any current or future media, including reprinting/republishing this material for advertising or promotional purposes, creating new collective works, for resale or redistribution to servers or lists, or reuse of any copyrighted component of this work in other works.

Design of a Position-Independent End-to-End Inductive WPT link for Industrial Dynamic Systems

Alex Pacini, Alessandra Costanzo
Dept. of Electrical,
Electronic and Information Engineering
"Guglielmo Marconi",
University of Bologna, Italy

Samer Aldhaher, Paul D. Mitcheson
Dept. of Electrical and Electronic Engineering,
Imperial College, London

***Abstract*—This paper will present the design of a position-independent inductive wireless power transfer (WPT) system for dynamic applications, where power is required to be delivered to a moving object on a path, such as industrial sliders and mass movers. A key feature of the designed inductive WPT system is to inherently maintain a constant dc output voltage, dc output power and dc-to-dc efficiency of the overall system, regardless of the vehicle's position. The system consists of an array of transmitting coils, where each coil is driven by a 6.78 MHz constant amplitude current generated from a load-independent Class EF inverter. The receiving coil is series tuned and is connected to a Class EF2 rectifier, which is numerically optimised to maintain a constant dc output, independently of the dc load. The system is powered from a 70V dc voltage source. GaN FET and SiC diodes are used to implement the Class EF inverter and rectifier. Results show a peak dc-dc efficiency of 83% at 150W with a 4% variation of the output voltage. The prototype of the complete link is under way.**

***Index Terms*—WREL, Inductive Powering, Position Independent, Sliding WPT.**

I. Introduction

Transport and industry rely on machinery and tools for a wide range of processes and applications. Delivering power using cables to moving machines and tools can constrain their freedom of movement. In addition, a common failure mechanism in many applications is cable degradation and loose connectors, which occur due to wear and tear from the repeated mechanical stress and pressure. Inductive Wireless Power Transfer (WPT) can be a solution to improve the reliability and functionality, as the use of cables and connectors are significantly reduced.

A key aspect to implement an inductive WPT system, is the ability to maintain a constant operation over a wide range of coil separations and variations of the load. Additionally, the WPT system should provide a regulation of the output voltage and maintain the variation of the generated magnetic field at the receiver within a certain limit, regardless of any change in the system. These challenges are yet to be overcome. Indeed, the majority of the works in literature show excellent overall system efficiency, however with fixed geometries and load.

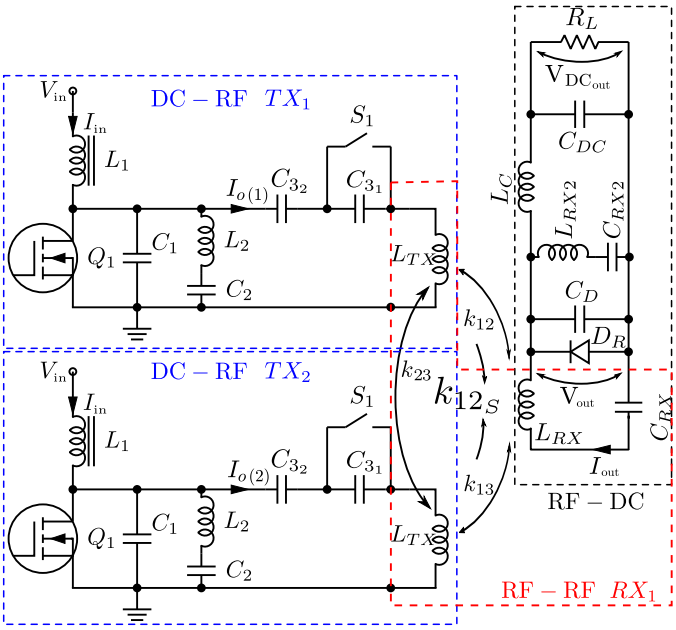


Fig. 1. Circuit schematic of the periodic dc-dc sliding WPT system. Two dc-RF converters are shown: their mutual coupling is outlined, together with the coupling to the receiver side. Only for subsection II-B, the RF output is loaded by a resistive load ($V_{out}/I_{out} \in \Re$)

In [1], the effects of a layout optimization on two coils connected in series and parallel are proposed, proving that there is a certain layout geometry of the RX coil which is able to stabilise the coupling factor while sliding in a linear direction. A further step is done in [2], by extending the previous results to more distances, showing that the series connection is still able to maintain a constant coupling factor. The work then measures an inductive resonant RF-to-RF WPT link composed of two transmitters and a receiver, operating at the resonance frequency of 6.78MHz, which is able to maintain the variations of efficiency and output voltage below 4%. A constant inductive resonant RF-RF WPT link can thus be obtained just by a series connection of two geometry optimised coils.

Both works focuses on the RF-to-RF link, without taking the hassle to implement the inverter and rectifier, being out of their scope. Although a conceptual switching scheme to achieve the series connection is proposed in [2], it has some drawbacks and it is still RF-to-RF.

The work in this paper will focus on the design of a complete Inductive Power Transfer (IPT) system, from the dc voltage source to the dc voltage output. The working frequency, designed to be in the MHz range to reduce the size of the inductors, is selected to be 6.78 MHz and the system is suitable for power levels around few hundred of Watts.

For the RF-to-RF link, the approach is derived to what is introduced in [1] but focusing on the series connection which, as suggested by [2], is performing better in more conditions.

For powering the transmitter side, we choose a Class EF Inverter acting as a constant sinusoidal current source, similar to the one in [3]. The key feature of this inverter topology is to obtain a fixed output current, which allows the active transmitting coils to be driven with an equal amplitude and phase current, thus enabling a virtual series connection and hence enforcing the theoretical framework developed in the previously mentioned works, but without having the hassle of the network in [2]. In this way, the system is unaffected by the stray inductances of the feeding lines. The advantage is extremely consistent with relatively high frequencies, as is with 6.78MHz, where the inductances of the feeding lines can change sensibly the resonance frequency. With this new design, the TX part of the link, that is the dc-to-RF sub-system, is composed by parallel connecting identical modules, where each one is composed of an inverter, with the same dc source, and a coil, allowing a fully modular and periodic system. The disadvantage is the need of multiple inverters, which could be blocking with higher powers. In those cases, an approach based on a low frequency AC feed may be better suited, which could be derived from the network proposed in [2] and taking care of the possible drawbacks.

The rectifier is numerically optimised connected to the entire system, in order to ensure the proper terminations of the EF class inverters. Indeed, this kind of inverter is able to cope with resistance variations only and is rather sensitive to reactance variations. The rectifier topology adopts a Class E configuration similar to the one proposed in [4], modified to a Class EF2 [5] in order to obtain a larger number of design variables needed for the optimum solution.

The final design is a practically constant sliding link with a constant output dc voltage over a quite large range of possible loads.

II. Design of the Dc-RF Sliding Link

A. Coupled Class EF Inverter Current Sources

Let us consider a single standalone Class EF Inverter solution, acting as a current source [3]. This topology is able to maintain a zero-voltage switching (ZVS) operation, while producing a constant output current, for a wide load range and without any re-tuning or components replacement.

A useful feature of this inverter, if adopted for a distributed implementation of a WPT system, is its ability to obtain a constant RF output current, which allows to force the same current through each transmitting coil, thus enabling a virtual series connection, as suggested in [2]. The link operating frequency is 6.78 MHz, which requires a transmitting coil of 1.3146 μH (see Fig. 2 for a sketch of the system which shows the coils). The circuit components of the inverter have

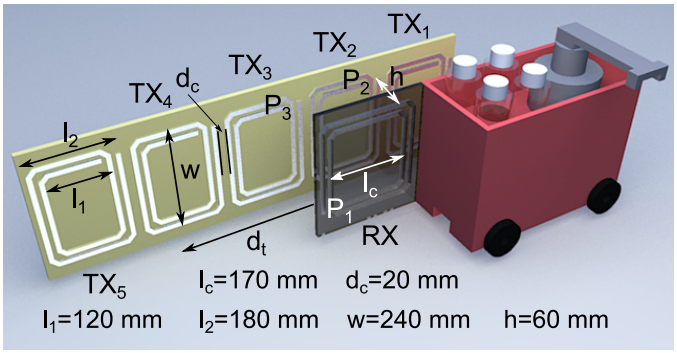


Fig. 2. Example of the system, where only two Tx are active at each time.

been obtained by a numerical solution and the resulting values are: $L_1 = 100\mu H$ (RF Choke), $L_2 = 282.86nH$, $C_1 = 920pF$, $C_2 = 698.5pF$, $C_3 = 540pF$, duty-cycle $D = 0.3$. In such conditions, the proper inverter load is bounded between 0 and 6 Ohm [3]. For a sliding WPT system, the coupling between the inverters need be accounted and the stand-alone topology can be used only as the starting point. Indeed, when two nearby transmitting coils are powered, the effect of the coupling between them results in a reduction of the effective inductance, that can be evaluated as:

$$L_3^{'} = L_3 \left(1 + k_{23}\right). \tag{1}$$

The latter can be calculated by a straightforward application of the V-I relationship of the three-port network, representing the RF-RF link of Fig. 1 and Fig. 2. For this RF-RF link, the coupling between the TX coils, located at a distance of 60mm, k_{23} results to be -0.0595. The inductance is therefore smaller and the proper compensating capacitor, which provides the same residual inductance to the inverter loaded with the equivalent inductance $L_3^{'}$, is:

$$C_3^{'} = \frac{C_3}{1 + \left(\frac{\omega}{\omega_{res}}\right) k_{23}}, \text{ where } \omega_{res} = \frac{1}{\sqrt{C_3 L_3}}. \tag{2}$$

C_3 is the optimal value for the stand-alone inverter [3].

Furthermore, the currents circulating in the powered coils induce a current in the non powered ones (not shown in Fig. 1). From simulations, this current is estimated to be of the same order of the desired ones, thus introducing significant contributions in terms of losses. To mitigate this undesired effect, the capacitor C_3 is split in two and a switch (S_1 in Fig. 1) is inserted in parallel to the smallest capacitor: if the inverter is off, the switch is closed, if the inverter is on, the switch is open.

With this configuration the resonance of the non powered loop is significantly modified, and its current is reduced by a factor of ten.

The series of the two capacitor is set to be equal to the total desired value of C_3, while the rationale to select which one to short is based on maximising the variation of the resonance frequency when the switch S_1 is closed. The relations are shown in Eq.s (3).

$$C_{3_2} = \alpha C_{3_1}$$

$$C_{3_1} = C_3 \left(\frac{\alpha + 1}{\alpha} \right) \tag{3a}$$

$$C_{3_2} = C_3 \left(\alpha + 1 \right) \tag{3b}$$

B. Position Independent Dc-to-RF link

To evaluate the dc-RF link for different sliding positions, the RF receiver side is firstly loaded by a resistive load. This allows us to preliminary control the simultaneous operation of the coupled inverters and to check the ability of maintaining the same RF current, and thus their virtual series connection.

Fig. 3 shows the inverter output currents through each respective coil for several relative position of the sliding receiver: these plots are almost indistinguishable. Fig. 3 also shows the inverters output RF voltages that are again superimposed. For the RX side the corresponding circuit components are: $L_{RX} = 1.6\mu H$, $C_{RX} = 344.4pF$. k_{12} and k_{13} are derived by the S-parameter measurements of the RF-RF link.

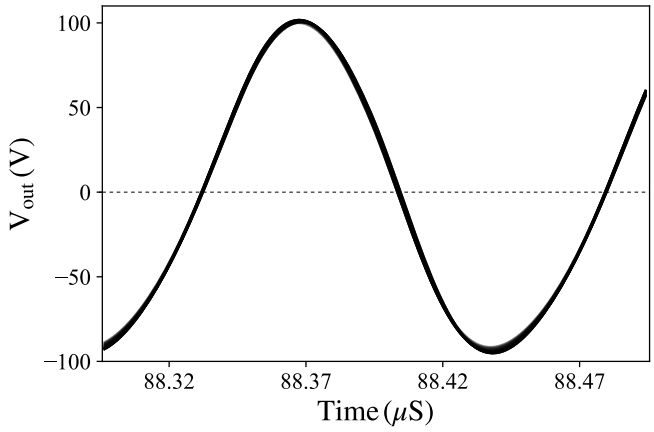


Fig. 3. RF output voltage (see Fig. 1) on the TX coils using a 70V DC source. The RF load is 40 Ohm. The lines are for 20 different positions, starting with the RX coil aligned to the first TX coil and ending with the RX coil in the middle of the two TX coils (from the middle to the second TX coil the behaviour is perfectly symmetric).

III. DC-DC Position Independent Link

The final dc-to-dc link system, which includes the rectifier, is shown again in Fig. 1. From that, the entire sliding WPT structure can be derived as a periodic replica, with the non-powered transmitters having the S_1 switch closed.

The design of a resonant rectifier, capable of behaving as voltage source and having a constant input reactance, is not straightforward. Since the whole circuit is based on multiple non-linearities, we designed the outline and then optimised the rectifier using a non-linear simulation of the whole system. For this purpose the Harmonic Balance technique was adopted, with 16 harmonics, to describe the non-linear regime: the system performances were also checked by time-domain simulation and they were in very good agreement, while reducing the computational time by three orders of magnitude.

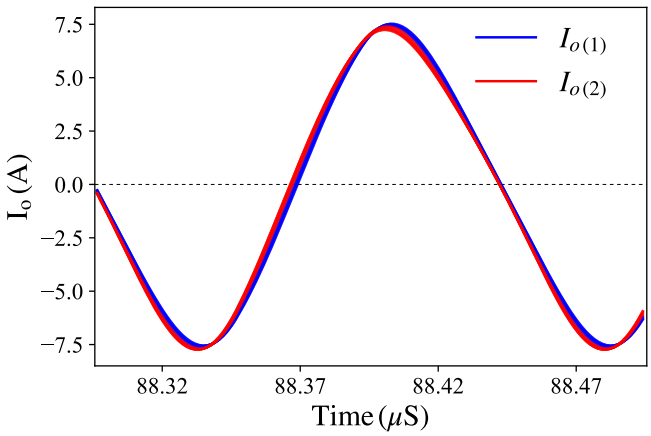


Fig. 4. RF currents I_0 (see Fig. 1) on the TX coils using a 70V DC source. The RF load is 40 Ohm. The lines are for 20 different positions, starting with the RX coil aligned to the first TX coil and ending with the RX coil in the middle of the two TX coils (from the middle to the second TX coil the behaviour is perfectly symmetric).

A recent work on a quasi-resistive input rectifier is presented in [4], where they designed a Class E Resonant Rectifier that maintains a near-resistive input impedance, but at the cost of a sensible output current ripple. Furthermore, the output voltage is strongly dependent on the load resistance, which is different from the required voltage source behaviour of the output.

For the design of the rectifier, we start from this topology and, to reduce the output current ripple, we increase the output RF choke inductor and add a RF shunt capacitor. Unfortunately, the degree of freedom were not yet sufficient for the optimisation to reach a satisfying performance. Then, by adding a series resonator in parallel, tuned on the second harmonic, and optimising again the whole system with the same goal, we were able to reach a good solution. The resulting rectifier topology can be classified as a Class EF2 [5].

The choice for the diode, which needs to have a relatively high current/voltage capability and, more importantly, low capacitance, is the Wolfspeed C3D1P7060Q. To sustain current peaks, four diodes are connected in parallel, which is possible being SiC diodes, and included in the simulation using their SPICE model.

Fig. 5 shows the DC output voltage, Fig. 6 the DC output power and Fig. 7 the overall dc-dc efficiency. Using an input source of 70V, the output DC power is 150W on a 40 Ohm load with a dc-dc efficiency of 82%. The voltage variation is under 4% for any load value over 30 Ohm, which is quite remarkable.

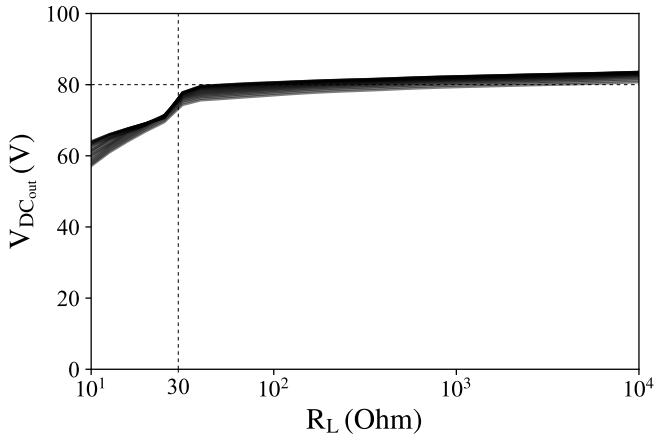


Fig. 5. Variation of the DC output voltage. The lines are for 20 different positions, starting with the RX coil aligned to the first TX coil and ending with the RX coil in the middle of the two TX coils.

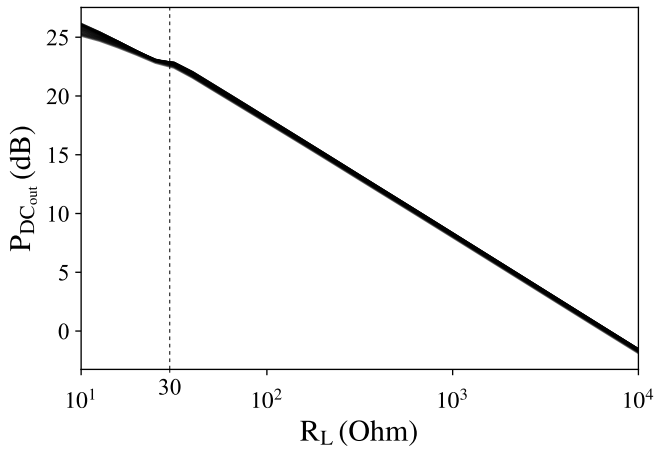


Fig. 6. Variation of the DC output power. The lines are for 20 different positions, starting with the RX coil aligned to the first TX coil and ending with the RX coil in the middle of the two TX coils. Since they are practically superimposed, we can affirm that the power variation with the same load is minimum. A 70V source gives 185W in the output.

The value of the other components are: $L_{RX} = 1.6\mu H$, $C_{RX} = 344.4pF$, $C_D = 30pF$, $C_{RX2} = 172pF$, $L_{RX2} = 0.8\mu H$, $L_C = 16\mu H$, $C_{DC} = 10\mu F$. The losses, expressed as a series resistance, are: $R_{L2} = 0.1\Omega$, $R_{L3} = 0.3\Omega$, $R_{LRX} = 0.3\Omega$, $R_{LRX2} = 0.1\Omega$, $R_{LC} = 0.1\Omega$. The other components are ideal.

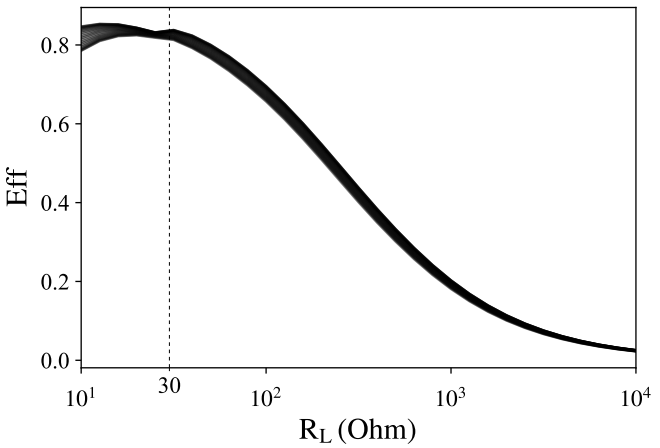


Fig. 7. Variation of the dc-dc efficiency. The lines are for 20 different positions, starting with the RX coil aligned to the first TX coil and ending with the RX coil in the middle of the two TX coils. Since they are practically superimposed, we can affirm that the efficiency variation with the same load is minimum. The dc-dc peak efficiency is 83% with 185W in the output.

REFERENCES

[1] A. Pacini, F. Mastri, R. Trevisan, A. Costanzo, and D. Masotti, "Theoretical and experimental characterization of moving wireless power transfer systems," in *2016 10th European Conference on Antennas and Propagation (EuCAP)*. Institute of Electrical and Electronics Engineers (IEEE), apr 2016. [Online]. Available: http://dx.doi.org/10.1109/EuCAP.2016.7481913

[2] A. Pacini, F. Mastri, R. Trevisan, D. Masotti, and A. Costanzo, "Geometry optimization of sliding inductive links for position-independent wireless power transfer," in *2016 IEEE MTT-S International Microwave Symposium (IMS)*. Institute of Electrical and Electronics Engineers (IEEE), may 2016. [Online]. Available: http://dx.doi.org/10.1109/MWSYM.2016.7540073

[3] S. Aldhaher, P. D. Mitcheson, and D. C. Yates, "Load-independent class EF inverters for inductive wireless power transfer," in *2016 IEEE Wireless Power Transfer Conference (WPTC)*, no. 1. Institute of Electrical and Electronics Engineers (IEEE), may 2016, pp. 1–4. [Online]. Available: http://dx.doi.org/10.1109/WPT.2016.7498864

[4] J. A. Santiago-Gonzalez, K. M. Elbaggari, K. K. Afridi, and D. J. Perreault, "Design of class e resonant rectifiers and diode evaluation for VHF power conversion," *IEEE Transactions on Power Electronics*, vol. 30, no. 9, pp. 4960–4972, sep 2015. [Online]. Available: http://dx.doi.org/10.1109/TPEL.2015.2398848

[5] S. Aldhaher, D. C. Yates, and P. D. Mitcheson, "Design and development of a class EF2 inverter and rectifier for multimegahertz wireless power transfer systems," *IEEE Transactions on Power Electronics*, vol. 31, no. 12, pp. 8138–8150, dec 2016. [Online]. Available: http://dx.doi.org/10.1109/tpel.2016.2521060